Magneto-optic parametric oscillation

Fredrik Jonsson

Department of Physics, The Royal Institute of Technology, S-100 44 Stockholm, Sweden

Christos Flytzanis

Laboratoire d'Optique Quantique, Ecole Polytechnique, F-911 28 Palaiseau Cedex, France

Received February 22, 2000

We develop a model of large-signal steady-state magneto-optic parametric oscillation in the Faraday configuration of a singly resonant cavity. The conversion efficiency and the threshold and phase-matching conditions are discussed, and we show that tunable phase matching can be achieved by use of a static magnetic field, eliminating any walk-off effects. © 2000 Optical Society of America

OCIS codes: 190.4970, 190.4360, 230.3810.

Optical parametric processes such as amplification and oscillation, which rely on the splitting of a photon of energy $\hbar\omega_3$ into two photons of lesser energies, $\hbar\omega_1$ and $\hbar\omega_2$, such that $\omega_3 = \omega_1 + \omega_2$, in bulk media depend critically on the phase-matching condition $\mathbf{k}_3 = \mathbf{k}_1 + \mathbf{k}_2$. This condition can be satisfied[1] by exploitation of the linear birefringence of anisotropic noncentrosymmetric media such as ferroelectric compounds, with concomitant complications: spatial walk-off and restrictions on polarization states and also in tunability range and the tunability scheme that is used.

Some of these problems can be circumvented by use of circularly birefringent crystals lacking inversion symmetry, where the relation between the electric induction and electric field is $\mathbf{D}_\omega = \epsilon_0(\epsilon : \mathbf{E}_\omega + i\mathbf{E}_\omega \times \mathbf{g})$, with ϵ being the dielectric constant, a scalar in the case of an isotropic medium, and $\mathbf{g}$ is the gyration vector. The case of magneto-optic parametric amplification was recently analyzed[2]; here we extend this analysis to the case of a magneto-optic parametric oscillator (MOPO).

Schematically this device consists of a noncentrosymmetric magneto-optic dielectric placed between two partially reflecting plane surfaces, separated by a distance L, in the Faraday configuration, with the optical fields propagating collinearly along the direction of the externally applied static magnetic field $\mathbf{H}_0 = H_0\mathbf{e}_z$. To make the points clear we have chosen to analyze a setup with the optical waves propagating in the [111] direction (laboratory z axis) of a crystal of point-symmetry class $\overline{4}3m$, which includes most heteropolar semiconductors; we recall that in such compounds the conventional phase-matching scheme is not operational. With the magnetic field switched on, the left-circularly polarized (LCP) and right-circularly polarized (RCP) waves of the same frequency experience different refractive indices, $n_k^{\pm} = n_k \pm \gamma_k/2n_k$, which are split by an amount γ_k/n_k that depends on the magnetic field and the magneto-optic coupling strength. Accordingly, phase matching by dispersion compensation can be achieved with a proper combination of circular polarizations for the pump, signal, and idler waves.

We introduce the circularly polarized basis $\mathbf{e}_\pm = (\mathbf{e}_x \pm i\mathbf{e}_y)/\sqrt{2}$ and separate the electric fields into circularly polarized components labeled $\pm$ for each frequency, or $\omega_3 = \omega_1^{\pm} + \omega_2^{\pm}$ with $\omega_3 = \omega_3^{\pm}$. Keeping only the lowest-order optical and magneto-optic nonlinearities, using the constitutive relations and wave equation (1) of Ref. 2, we find that the involved fields inside the cavity are resolved into forward- and backward-traveling components according to

$$E_{\omega_k}^{\pm} = E_{\omega_k}^{f\pm} \exp(i\omega_k^{\pm} n_k z/c) + E_{\omega_k}^{b\mp} \exp(-i\omega_k^{\pm} n_k z/c),$$

where $E_{\omega_k}^{\pm} = \mathbf{e}_{\pm}^{*} \cdot \mathbf{E}_{\omega_k}$. The boundary conditions of the cavity are at $z = 0$ and $z = L$:

$$E_{\omega_k}^{f\pm}(0) = \tau_{\pm}^{(0)}(\omega_k) E_{\omega_k}^{I\pm} + \rho_{\mp}^{(0)}(\omega_k) E_{\omega_k}^{b\mp}(0), \qquad (1a)$$

$$E_{\omega_k}^{b\pm}(L) = \rho_{\pm}^{(1)}(\omega_k) E_{\omega_k}^{f\pm}(L) \exp(2i\omega_k^{\pm} n_k L/c), \qquad (1b)$$

$$E_{\omega_k}^{T\pm} = \tau_{\pm}^{(1)}(\omega_k) E_{\omega_k}^{f\pm}(L) \exp(i\omega_k^{\pm} n_k L/c), \qquad (1c)$$

where $E_{\omega_k}^{I\pm}$ and $E_{\omega_k}^{T\pm}$ are the incident and the transmitted fields, respectively, and $\tau_{\pm}^{(0,1)}(\omega_k)$ and $\rho_{\pm}^{(0,1)}(\omega_k)$ are the complex amplitude transmission and reflection coefficients, respectively, as given explicitly in Ref. 3, when temporal dispersion and lowest-order magneto-optic interaction are taken into account.

Below we restrict the theory to a singly resonant cavity, which is transparent for the idler and the pump waves, for which $\rho_{\pm}^{(0,1)}(\omega_k) = 0$ and $\tau_{\pm}^{(0,1)}(\omega_k) = 1$, where $k = 1, 3$, and $E_{\omega_k}^{I\pm} = 0$, where $k = 1, 2$. When we take new real and positive variables $u_k^{\pm}$, $v_k^{\pm}$, $\varphi_k^{\pm}$, and $\psi_k^{\pm}$, according to the ansatz

$$E_{\omega_k}^{f\pm}(z) = [C_k^{\pm} u_k^{\pm}(z)]^{1/2} \exp[i\varphi_k^{\pm}(z) \pm i\omega_k^{\pm}\gamma_k z/(2n_k c)],$$

$$E_{\omega_k}^{b\pm}(z) = [C_k^{\mp} v_k^{\pm}(z)]^{1/2} \exp[i\psi_k^{\pm}(z) \pm i\omega_k^{\mp}\gamma_k z/(2n_k c)],$$

where $C_k^{\pm}$ are normalization constants with magnitudes determined by the optical and magneto-optic nonlinearities of the medium,[2] and where the parameters γ_k are the magneto-optic gyration constants, which are directly proportional to the magnetic field H_0, after applying the slowly varying envelope

0146-9592/00/171249-03$15.00/0

approximation we obtain the set of equations for the forward-traveling intracavity waves:

$$\frac{\partial u_1^{\pm}}{\partial z} = \frac{\partial u_2^{\pm}}{\partial z} = -\frac{\partial u_3^{\mp}}{\partial z} = -2|\kappa_{\pm}|(u_1^{\pm}u_2^{\pm}u_3^{\mp})^{1/2}\sin\theta_{\pm}, \tag{2a}$$

$$\frac{\partial \theta_{\pm}}{\partial z} = \Delta\beta_{\pm} \mp \Delta\alpha_{\pm} + \frac{1}{2}\cot\theta_{\pm}\frac{\partial}{\partial z}\ln(u_1^{\pm}u_2^{\pm}u_3^{\mp}), \tag{2b}$$

where Eqs. (2a) constitute the Manley–Rowe relation, reflecting conservation of energy flow in the forward direction, and the backward-traveling intracavity waves are described by

$$v_{2\mp}(z) = |\rho_{\pm}^{(1)}(\omega_2)|^2 u_2^{\pm}(L), \qquad v_{1\mp}(z) = v_{3\mp}(z) = 0,$$
$$\psi_{2\mp}(z) = \arg\rho_{\pm}^{(1)}(\omega_2) + \varphi_2^{\pm}(L),$$

where $\kappa_{\pm}^2 = C_1^{\pm}C_2^{\pm *}C_3^{\mp}$, and where we define

$$\Delta\beta_{\pm} = (\omega_3 n_3 - \omega_2^{\pm}n_2 - \omega_1^{\pm}n_1)/c,$$
$$\Delta\alpha_{\pm} = (\omega_1^{\pm}\gamma_1/n_1 + \omega_2^{\pm}\gamma_2/n_2 + \omega_3\gamma_3/n_3), \tag{2c}$$

and the relative phase angle

$$\theta_{\pm} = (\Delta\beta_{\pm} \mp \Delta\alpha_{\pm})z + \varphi_3^{\mp} - \varphi_2^{\pm} - \varphi_1^{\pm} + \arg\kappa_{\pm}.$$

From Eqs. (2), the pump wave obeys

$$\frac{1}{4|\kappa_{\pm}|^2}\left(\frac{\partial u_3^{\mp}}{\partial z}\right)^2 = (u_3^{\mp} - u_{3a}^{\mp})(u_{3b}^{\mp} - u_3^{\mp})(u_{3c}^{\mp} - u_3^{\mp}),$$

with $u_{3b}^{\mp} = u_3^{I\mp}$ as the input pump intensity and

$$u_{3a}^{\mp} = \frac{u_3^{I\mp}}{2}\{1 + s_{\pm}^2 + \phi_{\pm}^2 - [(1 + s_{\pm}^2 + \phi_{\pm}^2)^2 - 4\phi_{\pm}^2]^{1/2}\},$$

$$u_{3c}^{\mp} = \frac{u_3^{I\mp}}{2}\{1 + s_{\pm}^2 + \phi_{\pm}^2 + [(1 + s_{\pm}^2 + \phi_{\pm}^2)^2 - 4\phi_{\pm}^2]^{1/2}\},$$

where $s_{\pm}^2 = u_2^{\pm}(0)/u_3^{I\mp}$ is the signal-to-pump ratio and $\phi_{\pm} = (\Delta\beta_{\pm} \mp \Delta\alpha_{\pm})/[2|\kappa_{\pm}|(u_3^{I\mp})^{1/2}]$ is the dimensionless normalized phase mismatch. This equation can now be integrated in terms of Jacobian elliptic functions,[4] and, using the Manley–Rowe relations, we give the envelopes of the forward-traveling intracavity fields as

$$u_1^{\pm}(z) = u_3^{I\mp} - u_3^{\mp}(z), \tag{3a}$$

$$u_2^{\pm}(z) = (1 + s_{\pm}^2)u_3^{I\mp} - u_3^{\mp}(z), \tag{3b}$$

$$u_3^{\mp}(z) = u_{3a}^{\mp} + (u_{3b}^{\mp} - u_{3a}^{\mp}) \times \mathrm{sn}^2[|\kappa_{\pm}|(u_{3c}^{\mp} - u_{3a}^{\mp})^{1/2}z - K(\xi_{\pm}), \xi_{\pm}], \tag{3c}$$

where the modulus $\xi_{\pm}$ of the elliptic functions is given as

$$\xi_{\pm}^2 = \frac{1 - s_{\pm}^2 - \phi_{\pm}^2 + [(1 + s_{\pm}^2 + \phi_{\pm}^2)^2 - 4\phi_{\pm}^2]^{1/2}}{2[(1 + s_{\pm}^2 + \phi_{\pm}^2)^2 - 4\phi_{\pm}^2]^{1/2}}.$$

In Eqs. (3), $K(\xi_{\pm})$ denotes the complete elliptic integral of the first kind.[4] One also obtains the phases of the signal and the idler envelopes as

$$\varphi_{1,2}^{\pm}(z) - \varphi_{1,2}^{\pm}(0) = \frac{(\Delta\beta_{\pm} \mp \Delta\alpha_{\pm})}{2}\int_0^z \frac{[u_3^{I\mp} - u_3^{\mp}(z)]}{u_{1,2}^{\pm}(z)}\mathrm{d}z.$$

Solutions (3) correspond to the classical solutions obtained in second-order electric–dipolar nonlinear optics,[5] and here they are extended to include magnetic–dipolar interactions as well.

By use of solutions (3) and $u_2^{\pm}(0) = R_{\pm}u_2^{\pm}(L)$, where $R_{\pm} = |\rho_{\mp}^{(0)}(\omega_2)\rho_{\pm}^{(1)}(\omega_2)|^2$ is the LCP–RCP signal cavity round-trip reflectance, the signal-to-pump ratio $s_{\pm}^2$ is then determined from

$$(1 - R_{\pm})s_{\pm}^2/R_{\pm} = \frac{1}{2}\{1 - s_{\pm}^2 - \phi_{\pm}^2 + [(1 + s_{\pm}^2 + \phi_{\pm}^2)^2 - 4\phi_{\pm}^2]^{1/2}\} \times \mathrm{cn}^2\{\zeta_{\pm}[(1 + s_{\pm}^2 + \phi_{\pm}^2)^2 - 4\phi_{\pm}^2]^{1/4} - K(\xi_{\pm}), \xi_{\pm}\}, \tag{4}$$

where $\zeta_{\pm} = (u_3^{I\mp})^{1/2}|\kappa_{\pm}|L$ is the dimensionless input pump intensity normalized to cavity length and material constants (characteristic interaction length). The cavity condition for the resonant signal is similarly obtained from the arguments of boundary conditions (1) as

$$2\frac{\omega_2^{\pm}n_2^{\pm}L}{c} + \varphi_2^{\pm}(L) - \varphi_2^{\pm}(0) + \arg[\rho_{\mp}^{(0)}(\omega_2)\rho_{\pm}^{(1)}(\omega_2)] = 2\pi m,$$

where m is any integer. The phase-matched signal and idler frequencies are determined by the phase-matching conditions $\Delta\beta_{\pm} \mp \Delta\alpha_{\pm} = 0$ as

$$\frac{\omega_2^{\pm}}{\omega_{20}} = \left[1 \mp \frac{(\gamma_3/n_3 + \gamma_1/n_1)}{2(n_3 - n_1)}\right] \Bigg/ \left[1 \pm \frac{(\gamma_2/n_2 - \gamma_1/n_1)}{2(n_2 - n_1)}\right],$$

where $\omega_{20} = (n_3 - n_1)\omega_3/(n_2 - n_1)$ is the phase-matched signal frequency in the absence of a static magnetic field.

The LCP and RCP threshold pump intensities are obtained from Eq. (4) in the small-signal limit, where $s_{\pm} \ll 1$, as

$$\cosh[(1 - \phi_{\pm}^2)^{1/2}\zeta_{\pm,\mathrm{th}}] = \left[\frac{1 - (1 - R_{\pm})\phi_{\pm}^2}{R}\right]^{1/2}. \tag{5}$$

The pump threshold versus normalized phase mismatch is shown in Fig. 1 for a set of signal reflectances. From Eq. (5), real solutions for the pump threshold require that $(1 - R_{\pm})\phi_{\pm}^2 \le 1$; the corresponding limiting boundaries in the $(\phi_{\pm}, \zeta_{\pm,\mathrm{th}})$ plane are shown by the dashed curves. The intracavity signal-to-pump ratio $s_{\pm}^2$ versus phase mismatch $\phi_{\pm}$ is shown in Fig. 2.

An important feature of the MOPO operation can easily be appreciated from this analysis, namely, that spatial walk-off does not appear anywhere because the circular birefringence does not cause angular separation of the LCP and RCP waves, contrary to the case

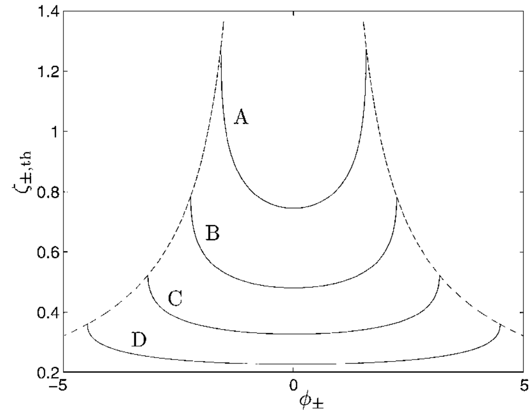

Fig. 1. Threshold pump $\zeta_{\pm,\mathrm{th}}$ versus normalized phase mismatch $\phi_\pm$ for values of $R_\pm \equiv |\rho_\mp^{(0)}(\omega_2)\rho_\pm^{(1)}(\omega_2)|^2$ of A, 0.6; B, 0.2; C, 0.9; and D, 0.95. The dashed curves indicate the limiting trajectories for real $\zeta_{\pm,\mathrm{th}}$.

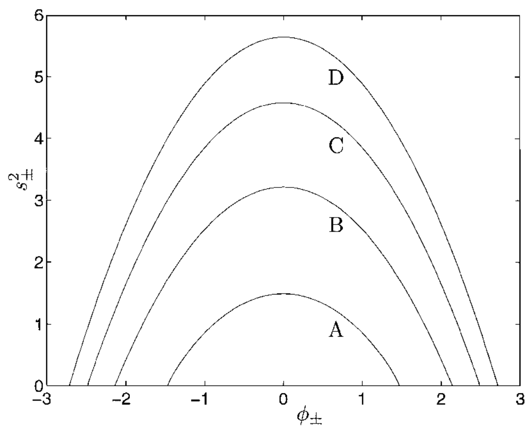

Fig. 2. Intracavity forward-traveling signal-to-pump ratio $s_\pm^2$ versus normalized phase mismatch $\phi_\pm$. $\zeta_\pm = 1$, and the values of $R_\pm$ are A, 0.6; B, 0.8; C, 0.9; D, 0.95.

of linear birefringence with ordinary and extraordinary waves in conventional optical parametric oscillator with anisotropic crystals.

Also correlated with this feature is the possibility of having a MOPO that uses an isotropic nonlinear crystal, as in the case of, for example, crystals belonging to the cubic point-symmetry class, e.g., $\bar{4}3m$, a case that is not possible in conventional optical parametric oscillator operation because of phase mismatch. This raises the possibility that one can use heteropolar semiconductors, which possess some of the highest values of second-order susceptibility $\chi^{(2)}$, at least an order of magnitude higher than those of the ferroelectrics and other oxygen-polyedra-based compounds that are currently used as optical parametric oscillator materials. This possibility has favorable repercussions for threshold condition and propagation analysis.

It is evident that application of a static magnetic field, besides providing the circular birefringence that one needs to achieve phase matching, through its control and variation also provides frequency-tunability control. This implies that materials with large magneto-optic coupling strength (Verdet constant) in the transparency range and, simultaneously, large values of second-order susceptibility should be chosen. Such a class of materials is that of the diluted magnetic semiconductors, e.g., $Cd_{1-x}Mn_xTe$ and similar magnetic impurity-doped II–VI semiconductivity compounds, in which a spin-exchange interaction[6] leads to giant Faraday rotations that still preserve the electronic structure of the undoped compound with its high value of $\chi^{(2)}$.

The transparency range of $Cd_{1-x}Mn_xTe$ extends up to 2 eV ($\lambda \sim 0.6\ \mu$m) and down to 0.06 eV ($\lambda \sim 16\ \mu$m), limited by the onset of band-to-band transitions and two-photon absorption, respectively; this transparency range sets the frequency range for the pump and the idler and signal (keep in mind that two-photon transitions may also be a limiting factor). The figures of merit of these materials seem favorable, and a rough estimate gives a 5% tunability range around the degenerate point, $\omega_1^\pm = \omega_2^\pm$, for magnetic field intensities up to $\sim$1 T.

Besides its potential and new device features, the MOPO will open the way to interesting studies into quantum optical effects with circular photon states in regard to quantum noise, twin-state interference and correlation, and other quantum magneto-optic aspects.

F. Jonsson's e-mail address is fj@optics.kth.se.

References

1. Y. R. Shen, *The Principles of Nonlinear Optics* (Wiley, New York, 1984).
2. F. Jonsson and C. Flytzanis, Opt. Lett. **24,** 1514 (1999).
3. F. Jonsson and C. Flytzanis, Phys. Rev. Lett. **82,** 1426 (1999).
4. P. F. Byrd and M. D. Friedman, *Handbook of Elliptic Integrals for Engineers and Scientists*, 2nd ed. (Springer-Verlag, Berlin, 1971).
5. J. A. Armstrong, N. Bloembergen, J. Ducuing, and P. S. Pershan, Phys. Rev. **127,** 1918 (1962); P. P. Bey and C. L. Tang, IEEE J. Quantum Electron. **QE-8,** 361 (1972).
6. J. K. Furdyna, J. Appl. Phys. **64,** R29 (1988).